Functionalised collagen spheres reduce H_2O_2 mediated apoptosis by scavenging overexpressed ROS

Christos Tapeinos[a], Aitor Larrañaga[a,b], Jose-Ramon Sarasua[b], Abhay Pandit[a,*]

[a] CÚRAM, Centre for Research in Medical Devices, National University of Ireland Galway, Ireland

[b] Department of Mining-Metallurgy Engineering and Materials Science & POLYMAT, University of the Basque Country, Bilbao, Spain

Email addresses: ctapeinos@gmail.com, aitor.larranagae@ehu.eus, jr.sarasua@ehu.es

Corresponding author: abhay.pandit@nuigalway.ie

Abstract

The excess of reactive oxygen species (ROS) has been related with numerous diseases including cancer, cardiovascular and neurodegenerative diseases. Overexpression of ROS can lead to oxidative stress and subsequently to H_2O_2-mediated cell apoptosis. In this study, it was demonstrated that biodegradable PLGA microspheres coated with collagen type I and decorated with MnO2 nanoparticles acted as ROS scavengers controlling the H_2O_2-mediated apoptosis of cells undergoing oxidative stress. The results showed that the functionalized collagen spheres can protect cells even in very harsh conditions of oxidative stress.

Keywords: PLGA, Collagen microspheres, ROS scavengers, MnO_2, apoptosis, oxidative stress

Word count for manuscript: 4890

Number of references: 30

Number of figures: 6

Number of tables: 0

This material is based upon works supported by the European Union funding under the 7th Framework Programme under Grant Agreement Number 317304.

This publication has emanated from research supported in part by a research grant from Science Foundation Ireland (SFI) and is co-funded under the European Regional Development Fund under Grant Number 13/RC/2073.

A. Larrañaga would like to acknowledge Basque Government (Department of Education, Language Policy and Culture) for funding his postdoctoral studies.

The Authors declare no competing interests

1. Background

Reactive oxygen species (ROS), such as hydrogen peroxide (H_2O_2), hydroxyl ($^{\cdot}OH$) and superoxide anion radicals ($^{\cdot}O_2^-$), are a family of reactive molecules that play a pivotal role in several cellular events among which are gene expression, transcription factor activation, DNA damage, cellular proliferation and apoptosis [1]. Under normal physiological conditions, ROS are efficiently regulated by a group of molecules and enzymes with antioxidant properties including glutathione, superoxide dismutase and catalase. At these low/moderate concentrations, ROS are beneficial and act as mediators of cellular signalling, proliferation and differentiation [2]. However, ROS overproduction can result in an imbalance in the metabolism of these reactive intermediates leading to oxidative stress. It is well known that oxidative stress can damage cellular structures (including lipids, membranes, proteins and DNA) leading to cellular apoptosis and senescence [3, 4].

With an awareness of the impact of oxidative stress in numerous disease pathologies (including cancer [5, 6], neurodegeneration [7] and diabetes [8]), there is a need to develop an efficient biomaterial-based drug delivery antioxidant system to control the concentration of ROS in the cellular microenvironment [9]. These therapeutic structures can take the form of nano/microparticles, polymer vesicles, hydrogels that either show inherent antioxidant properties or release encapsulated antioxidant molecules in a controlled manner due to their structural changes in response to a specific trigger [10-13].

Recently, the benefits of manganese dioxide nanoparticles (MnO_2 NPs) to simultaneously regulate the levels of H_2O_2 and to sustainably produce O_2 in a tumour microenvironment have been demonstrated [14-16]. MnO_2 NPs have several advantages over other metals and metal oxides. These advantages include the specific decomposition of H_2O_2 without the generation of hydroxyl radicals and the breakdown of MnO_2 after the reaction to Mn^{2+} ions and water, which is critical in therapeutic applications as it avoids the accumulation of nanoparticles in

the body [17, 18]. However, the small size associated with these nanoparticles can compromise their colloidal stability and subsequent circulation in the bloodstream. To overcome this problem, conjugation of MnO_2 NPs with several polymers and lipids has been proposed in the aforementioned reports [14-16]. Herein, MnO_2 NPs are employed to decorate the surface of poly(lactide-co-glycolide) (PLGA) microspheres coated with collagen. PLGA has been widely employed in the biomedical field due to its biodegradability, tuneable mechanical and degradation properties and processability [19]. In order to improve their biological properties and, simultaneously facilitate the incorporation of MnO_2 NPs, PLGA microspheres were cloaked with collagen. Collagen is the main extracellular matrix (ECM) component of many tissues and has been used in several promising applications (including as a cell delivery platform [20], as hollow spheres for nucleic acid delivery [21, 22], and as a conduit for neural regeneration [23]).

In this study it was hypothesized that functionalized PLGA microspheres coated with collagen and decorated with MnO_2 NPs would protect cells from oxidative stress because of their H_2O_2 scavenging capacity and will, therefore, reduce apoptosis (**Figure 1**). To accomplish this, MnO_2 NPs were first synthesized and subsequently incorporated on the surface of PLGA-collagen microspheres. PLGA-Col-MnO_2 microspheres were tested for toxicity on two cell lines (3T3 and MCF7). The functionalised microspheres were then tested for, their capacity to efficiently scavenge H_2O_2 by protecting 3T3 and MCF-7 cells from H_2O_2-induced apoptosis. The protective effect of PLGA-Col-MnO_2 microspheres was also evaluated on these cells for viability, apoptosis and cell death by flow cytometry.

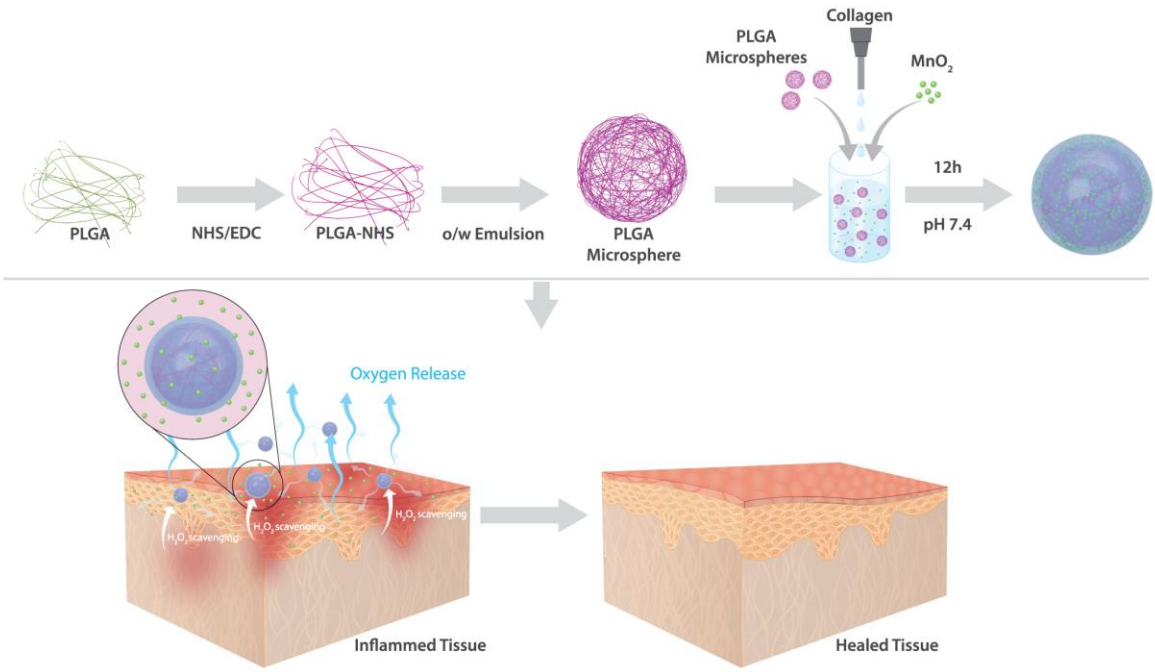

Figure 1: The schematic shows the experimental procedure of the fabrication of PLGA-Col-MnO_2 microspheres and the mechanism of action of these spheres on tissues that are under oxidative stress.

2. Methods

2.1.Materials

Resomer® RG 504 H; Poly(D,L-lactide-co-glycolide) (acid terminated, lactide:glycolide 50:50, M_w 38,000-54,000), N-(3-Dimethylaminopropyl)-N′-ethylcarbodiimide hydrochloride (EDC), N-Hydroxysuccinimide (NHS), Dichloromethane (DCM), Sodium hydroxide (NaOH), Phosphate buffer saline (PBS) (1x), H_2O_2 fluorometric assay kit and 2',7' – dichlorofluorescin diacetate (DCFDA) - Cellular Reactive Oxygen Species Detection Assay Kit were purchased from Sigma Aldrich. For cell culture, Dulbecco's Modified Eagle's Medium - high glucose (DMEM), Hanks' Balanced Salt Solution (HBSS), Fetal Bovine Serum (FBS), Penicillin Streptomycin (PS) were also purchased from Sigma-Aldrich. CellROX® Green Reagent used to measure oxidative stress, Quant-iT™ PicoGreen® dsDNA

Assay Kit used to measure the proliferation of the cells and AlamarBlue® Cell Viability Assay used to measure the cells' metabolic activity were all purchased from ThermoFisher Scientific. FITC Annexin V apoptosis detection kit was used for viability, early apoptotic and cell death studies by flow cytometry according to the manufacturer's protocol (BD Pharmingen, San Diego, CA, USA). Collagen type I from bovine tendon was extracted, purified and characterized as previously described [24, 25].

2.2.Methods

2.2.1. Activation of PLGA and microspheres fabrication

The activation of carboxylic acid terminated PLGA was carried out using NHS/EDC. The activated PLGA-NHS was used for the fabrication of microspheres using a homogenizer and an oil-in-water (O/W) emulsion method; *see supplementary information for detail.*

2.2.2. Morphological characterization of PLGA-Col-MnO_2 microspheres

The morphological characterization of the microspheres was carried out using a Hitachi Scanning Electron Microscope (SEM) with EDX Analysis System, at a working voltage and working current of 5kV and 10mA respectively and a Hitachi H7500 Transmission Electron Microscope (TEM) at working voltages 80 – 100 kV. The samples were coated with gold before their use in SEM and EDX. For the TEM analysis, the samples were dispersed in ethanol and were placed to either Agar Grids 200 Mesh Copper 3.05mm or Lacey Carbon Films on 200 Mesh Copper at working voltages 80 – 100 kV; *see supplementary information for detail.*

2.2.3. Physicochemical characterization of PLGA-Col-MnO_2 microspheres

The activated PLGA (PLGA-NHS) was characterized using nuclear magnetic resonance (NMR) on JEOL 400 MHz NMR ECX-400 Spectrometer. The structural characterization of the PLGA-Collagen microspheres and of manganese dioxide nanoparticles was carried out on a Varian 660-IR spectrometer operating in the ATR (Attenuated Total Reflectance) mode. The infrared absorption spectra for all the samples were collected at 25˚ C at a wavelength range from 4000 - 400 cm^{-1}. Sixteen scans with a resolution of 4 cm^{-1} were performed for each sample; *see supplementary information for detail.*

2.2.4. O_2 generation and H_2O_2 scavenging capacity of PLGA-Col-MnO_2 microspheres

Oxygen generation was measured using a Microx 4 trace fibre optic oxygen meter® with a PSt7-02 micro-sensor. Various concentrations of PLGA-Col-MnO_2 (100 μg/ml, 250 μg/ml and 500 μg/ml) were placed in a 1 ml airtight septum-cap glass vial with 0.5 ml of PBS (1x). The sensor was placed through the cap and left for five minutes for equilibration of O_2 inside the vial. Subsequently, 0.5 ml of various concentrations of H_2O_2 was added and data were collected every two seconds for 60 minutes. The data were collected using the Data Manager software of Presens® and analysed using OriginPro®.

The concentration of H_2O_2 before and after treatment with the PLGA-Col-MnO_2 microspheres was measured using an H_2O_2 fluorometric assay kit. Various concentrations of the microspheres (100 μg/ml, 250 μg/ml and 500 μg/ml) were placed in eppendorf tubes and incubated (shaking) at room temperature for fifteen minutes with various concentrations of H_2O_2. Subsequently, 50 μL of the supernatant were removed and were placed in a 96-well black plate with clear bottom. Then, 50 μL of a master mix solution containing a mix of the Amplex® Red reagent (10-acetyl-3,7-dihydroxyphenoxazine) and horseradish peroxidase, provided with the H_2O_2 assay kit was added in each well and incubated for twenty minutes at

room temperature. The readouts were measured using an enzyme-linked immunosorbent assay (ELISA) plate reader at λ_{ex} = 540/λ_{em} = 590 nm.

2.3. In vitro studies

2.3.1. Cell culture and treatments

3T3 rat fibroblast and MCF-7 breast cancer cell lines were cultured following standard cell culture procedures. Both cell lines were cultured in DMEM high glucose supplemented with 10% fetal bovine serum (FBS) and 1% penicillin /streptomycin (P/S) at 37º C in a humidified atmosphere, and the media was changed every two days. Cells were cultured until they reached 80% confluency before plating in 48 well-plates (Nunc Lab-Tek®). For all *in vi*tro experiments, cells were seeded in 48-well plates 24 hours prior to any treatment, at a cell density of 80,000 cells / cm^2. Cells were treated with various concentrations of PLGA-Col-MnO_2 microspheres (100 ug/ml, 250 ug/ml and 500 ug/ml) for different time points (6h, 24h and 48h) and various concentrations of H_2O_2 (100 μM, 500 μM and 1mM). All experiments were performed in triplicate (n=3).

2.3.2. Cell metabolic activity and proliferation

AlamarBlue® assay was used to measure the metabolic activity of the cells. The AlamarBlue® assay was carried out according to the manufacturer's instructions; *see supplementary information for detail.*

2.3.3. Apoptosis detection by flow cytometry

Both cell lines, 3T3 and MCF7, were stained with AnnexinV-FITC and propidium iodide (PI) according to the manufacturer's protocol for flow cytometry. Briefly, at each time point cells were washed with HBSS and detached using trypsin-EDTA (0.25%). A number of 20 $x10^5$

cell per tube were stained with 2 µl of Annexin V-FITC and 5 µl of PI in binding buffer (1x) for fifteen minutes at 37º C in the dark. Both cell lines stained with Annexin-V / PI were evaluated using a Beton-Dickinson FACS Canto Flow Cytometer (Mansfield, MA, USA). Live cells (Annexin V^- / PI^-), early apoptotic cells (Annexin V^+ / PI^-) and dead cells (PI^+) were analysed using FlowJo™ software 8.5.2 (Tree Star, Ashland, OR).

3. Results

3.1. Synthesis of MnO_2 nanoparticles and incorporation on the outer layer of PLGA/collagen microspheres

The MnO_2 NPs were synthesized using a simple one pot process as previously described in the literature[15, 16]. The resulting NPs had a spherical shape and size around 15 nm (*see supplementary information*: **Figure S1)**. Morphologically, the spheres were characterized using SEM and TEM. In **Figure 2**, the PLGA-NHS microspheres before and after coating with collagen and the embedding of MnO_2 nanoparticles, are shown. Before the coating (**Figure 2A**), the surface was smooth and a high polydispersity of the microspheres was observed. After the collagen coating and incorporation of the MnO_2 nanoparticles (**Figure 2B**), the surface of the PLGA-NHS spheres was altered, suggesting that the coating of the spheres had been successful. TEM analysis (**Figure 2C** and **Figure 2D**) showed that the spheres with a diameter greater than 1μm were hollow while spheres with a diameter of less than 1μm were not hollow This can be considered as an advantage as therapeutic molecules can be encapsulated within sphere's internal cavity. The stability of the PLGA-Col-MnO_2 microspheres was also assessed in *in vitro* media using DMEM with 10% FBS and 1% P/S, for 96 hours. No difference could be observed at the morphology and the structure of the microspheres as it can be seen in **Figure 2E**.

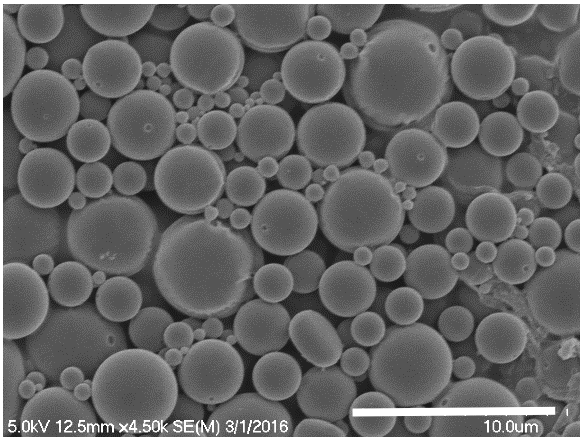

A

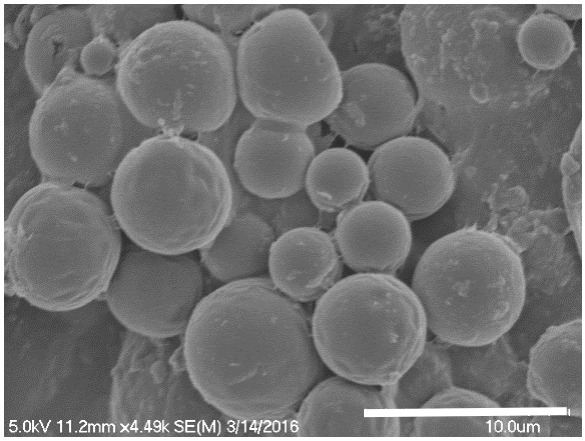

B

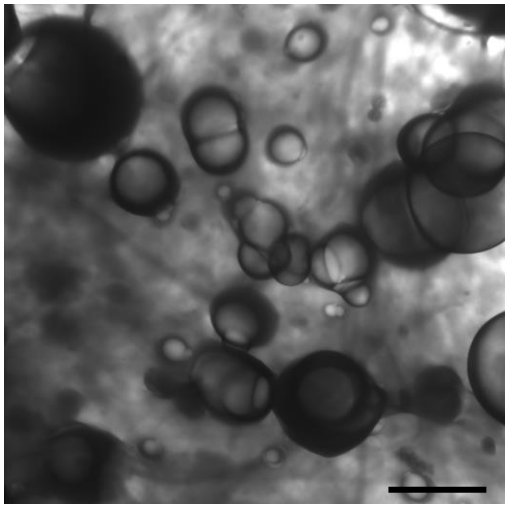

C

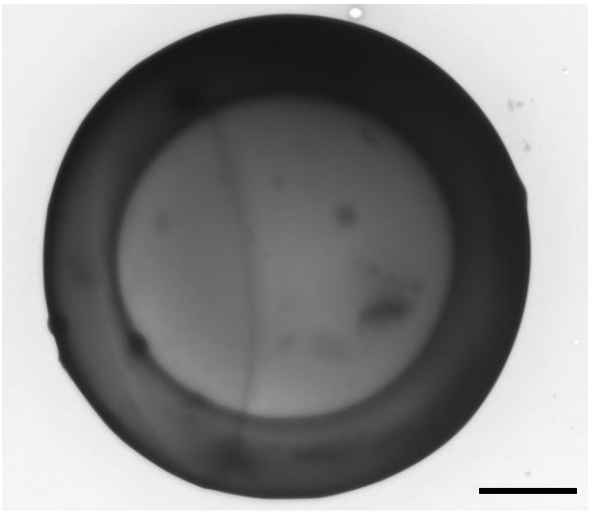

D

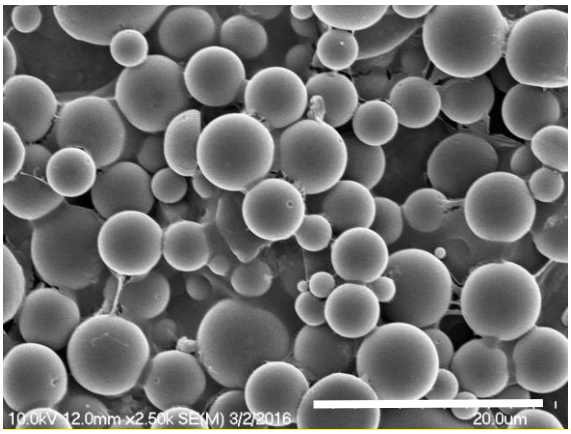

E

Figure 2: A) SEM image of activated PLGA microspheres. Scale bar: 10 μm; **B)** SEM image of PLGA-Col microspheres with embedded MnO_2 nanoparticles. Scale bar: 10 μm; **C)** TEM image of the PLGA-Col-MnO_2 microspheres. Scale bar: 2 μm; **D)** magnified TEM figure of a hollow PLGA-Col-MnO_2 microsphere after decoration with the MnO_2 nanoparticles. Scale bar: 1 μm. **E)** SEM image of PLGA-Col-MnO_2 microspheres after 96 hours in DMEM media with 10% FBS and 1% PS. Scale bar: 20 μm.

3.2. Oxygen generation and scavenging effect of the PLGA-Col-MnO_2 microspheres

MnO_2 nanoparticles can act either as a catalyst or as a reagent that fully reacts with H_2O_2 (**Eq. 1**), leading to its complete decomposition into manganese ions, water and oxygen. The

incorporation of the nanoparticles inside the microspheres protects the nanoparticles from being cleared by macrophages while in tandem it preserves the nanoparticles ability to scavenge H_2O_2 with the subsequent generation of O_2. Depending on the amount of PLGA-Col-MnO_2 microspheres and the concentration of H_2O_2, different amounts of generated oxygen was observed (**Figure 3)**. The highest amount of O_2 was generated (~4%) when the highest concentration of H_2O_2 (1 mM) reacts with the highest concentration of the microspheres (500 µg/ml) (**Figure 3A**) while the lowest oxygen generation (~0.5%) was observed when 100 µg/ml and 250 µg/ml of microspheres reacted with 50 µM of H_2O_2 (**Figure 3B**). It is evident from the results presented in **Figure 3** that O_2 generation can be controlled depending on the concentration of microspheres used.

$$MnO_2 + 2H_2O_2 \rightarrow Mn^{2+} + 2H_2O + 2O_2 \qquad (1)$$

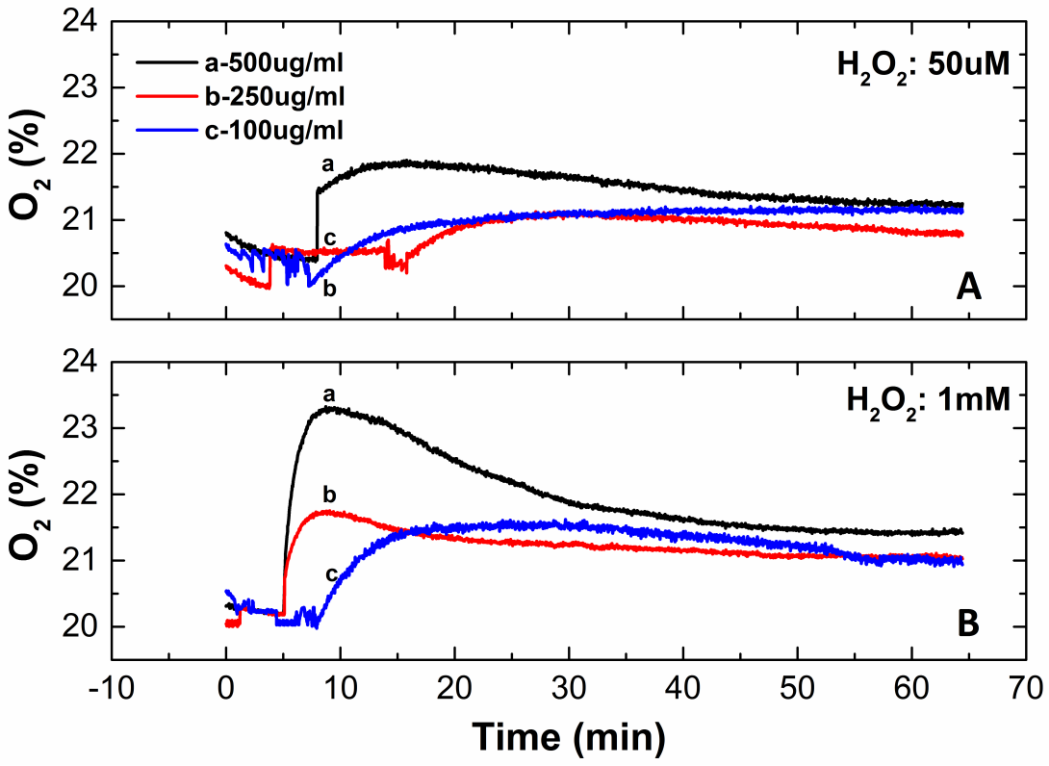

Figure 3: Oxygen generation after the reaction of various concentrations of PLGA-Col-MnO_2 microspheres with 50 µM H_2O_2 (biologically relevant endogenous concentration in

inflamed tissues) **(A)** and 1 mM (concentration used to mimic oxidative stress conditions) **(B)**.

The scavenging effect of the microspheres depends not only on their concentration but also on the amount of H_2O_2 that is used, as observed in **Figure 4**. Even for low concentrations of the microspheres (100μg/ml), the H_2O_2 concentration is reduced by approximately 30% when 50 μM H_2O_2 was used. Meanwhile, a reduction of approximately 50% was observed when in presence of 10 μM of H_2O_2. When the percentage of the microspheres was increased, the scavenging effect was enhanced. It is important to note that the scavenging effect was also dependent on the reaction time between the H_2O_2 molecules and the microspheres as the collagen layer prevents the direct reaction of the microspheres with the H_2O_2 molecules.

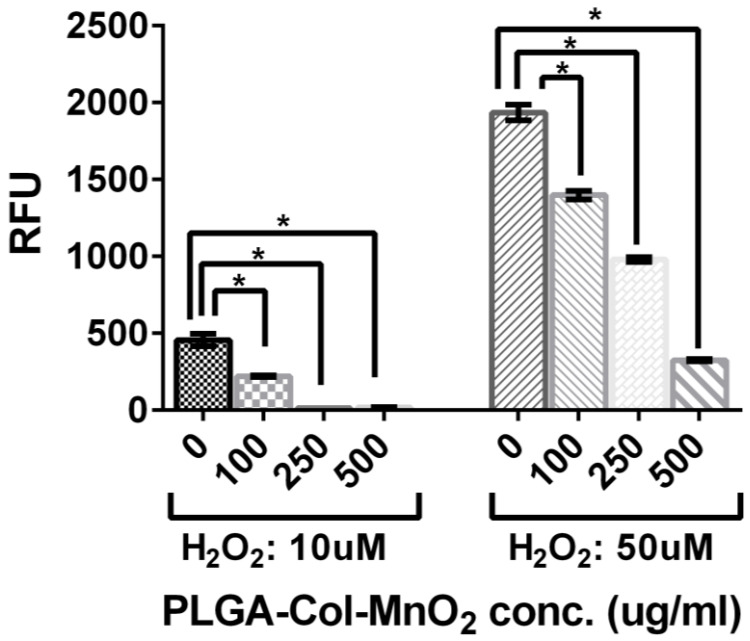

Figure 4: Scavenging effect of various concentrations of PLGA-Col-MnO_2 microspheres in the presence of 10 μM and 50 μM of H_2O_2 (n=3, ANOVA, *→$p<0.05$).

3.3. *In vitro studies*

A variety of assays were employed to prove the protective effect of the PLGA-Col-MnO_2 microspheres and their ability to reduce H_2O_2-mediated oxidative stress. Two different immortalized cell lines, 3T3 and MCF7, were used. Two different treatment regimens were studied: simultaneous treatment (Sim.Treat) and pre-treatment (Pre-treat). The Sim.Treat method involved the simultaneously addition of H_2O_2 and PLGA-Col-MnO_2 microspheres to cells while the Pre-treat method involved the pre-treatment of cells for one hour with H_2O_2 (1 mM) before adding a mixture of H_2O_2 (1 mM) together with the PLGA-Col-MnO_2 microspheres. Cells that were treated only with H_2O_2 (1 mM) acted as control. The rationale behind the pre-treatment experiments is to mimic the very harsh conditions of oxidative stress in tissues and thus to assess the efficacy of the PLGA-Col-MnO_2 microspheres to scavenge ROS in this harsh environment.

3.3.1. *Protective effect of PLGA-Col-MnO_2 microspheres on H_2O_2-induced DNA damage*

The effect of the PLGA-Col-MnO_2 microspheres on the cell proliferation rate was assessed using a DNA PicoGreen (PG) assay. The PG dye has the ability to bind to the double strand DNA helix and thus report the cell proliferation rate. The cells were treated with H_2O_2 either simultaneously with the microspheres or pre-treated for one hour before the addition of the microspheres. In addition, after pre-treating the cells for one hour the media was replaced with a fresh media containing 1mM H_2O_2, followed by the addition of the microspheres. This experiment was carried out in order to assess if the microspheres are able to protect cells even under very harsh conditions of oxidative stress.

In **Figure 5** where the results from 3T3 cells are illustrated it is evident that after six hours of treating cells only with 1 mM of H_2O_2 (the quantity of DNA was significantly less than the DNA amount in either simultaneous treatment (Sim.Treat) or Pre-treatment (Pre-treat) regimes. In addition, an increase in the proliferation of 3T3 cells was observed which was

independent of the microsphere concentration compared to cells treated only with H_2O_2 (**Figure 5A**). The rate of cell proliferation was lower in the pre-treated group compared to the simultaneous treated group when the same concentration of PLGA-Col-MnO_2 microspheres was used (**Figure 5A**). However, the use of 500 μg/ml microspheres in the H_2O_2 pre-treated group had some protective effect, presenting higher DNA amount compared to the cells treated only with H_2O_2. The reason why the pre-treated group presented a lower amount of DNA compared to the simultaneously treated group could be justified by the fact that the extremely high H_2O_2 concentrations that the cells are treated with, leads to cell death rendering the microspheres incapable of reversing this effect. Similar results were also observed for the MCF7 cells (**Figure 5B**) but a higher DNA amount was observed in MCF7 cells compared with 3T3 cells, when treated with 1 mM H_2O_2. This can be attributed to the fact that the mechanism by which cells experience oxidative stress is a cell type-dependent phenomenon and so also the mechanism by which microspheres protect cells from oxidative stress is cell-type dependent.

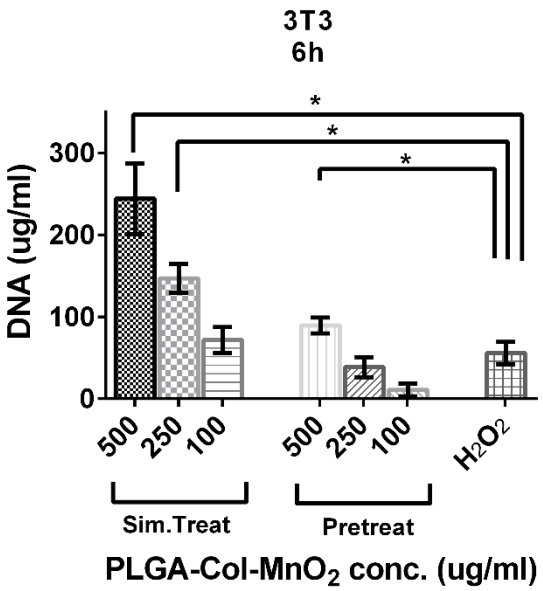

A

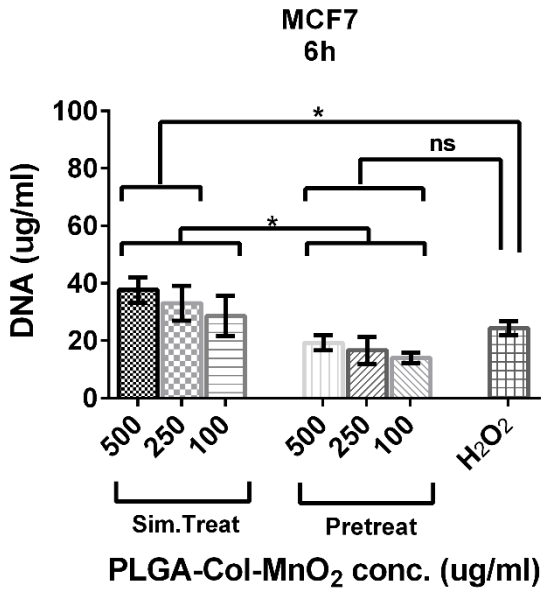

B

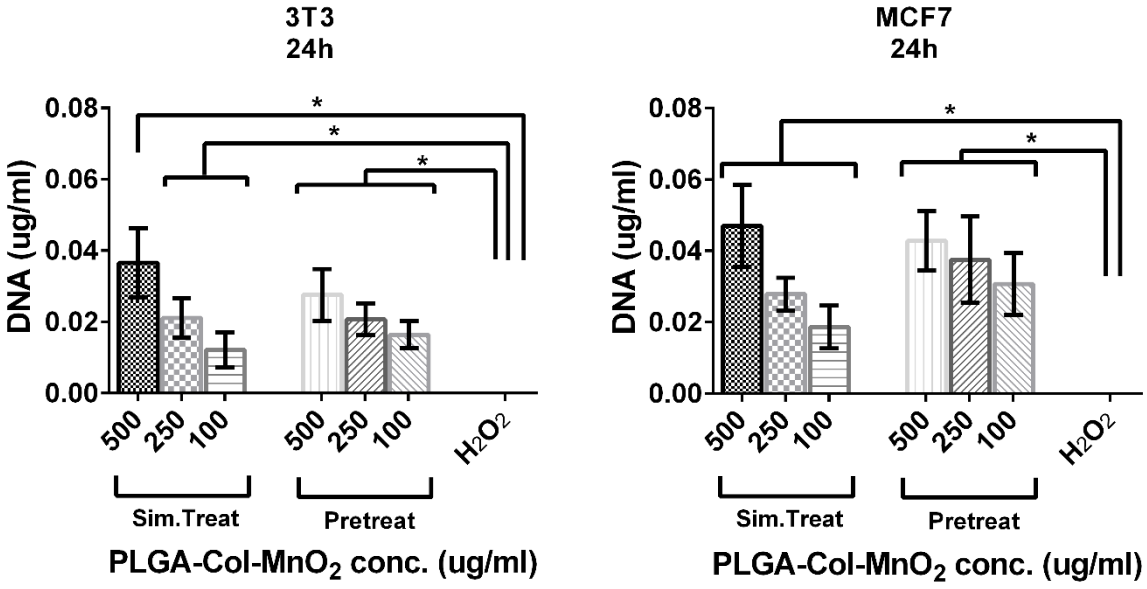

C **D**

Figure 5. DNA PicoGreen® assay on **A)** 3T3 and **B)** MCF7 cells undergoing oxidative stress by stimulation with 1 mM of H_2O_2 and under the Sim.Treat and Pre-treat treatment regimens with different concentrations (500μg/ml, 250μg/ml and 100μg/ml) of PLGA-Col-MnO_2 microspheres for 6h and **C)** 3T3 and **D)** MCF7 undergoing oxidative stress by stimulation with 1 mM of H_2O_2 and under the Sim.Treat and Pre-treat treatment regimens with different concentrations (500μg/ml, 250μg/ml and 100μg/ml) of PLGA-Col-MnO_2 microspheres for 24h. Significant difference was observed for 3T3 cells between stimulated group with 1 mM H_2O_2 and the Sim.Treat and Pre-treat groups (n=3, ANOVA, *→p<0.05).

After twenty-four hours, neither cell type that has been treated only with H_2O_2 exhibited any DNA content, due to the harsh environmental conditions. On the other hand, after twenty-four hours the groups treated with the microspheres (**Figure 5C** and **Figure 5D**) even though they present a considerably lower amount of DNA at twenty-four hours compared to six hours of treatment, they perform better demonstrating their protective effect against oxidative stress. These results prove that even in extreme conditions of oxidative stress, a

concentration of 500 μg/ml of PLGA-Col-MnO_2 microspheres can protect cells from immediate death.

3.4.*Protective effect of PLGA-Col-MnO_2 microspheres on H_2O_2-induced apoptosis*

To examine cell survival, both cell lines (3T3 and MCF7) in the presence of both treatments (simultaneous treatment and pre-treatment) were stained with Annexin V-FITC and PI and evaluated for viability, early apoptosis and cell death by flow cytometry as it can be seen in **Figure 6**. Across all treatments and controls respectively, data showed 80% viability, apart from MCF7 cells pre-treated with H_2O_2 where only 40% cell viability was observed. Cell apoptosis was evaluated by Annexin V as an early apoptotic marker. For the 3T3 cell line, both treatments result in increasing apoptotic cells (~15% for simultaneous treatment and ~9% for pre-treatment, in comparison with 1mM H_2O_2 (control ~5%). Data for the 3T3 cell line, from both treatments, suggest that there was an increasing trend in the number of cells undergoing apoptosis. However, after the analysis of cell death, the percentage of dead cells decreases for both treatments, simultaneous treatment (~6%) and pre-treatment (~12%) in comparison to the group that was treated only with 1mM of H_2O_2 (control~15%). For the MCF7 cell line the data suggests a diminished percentage of apoptotic cells (~3%) in comparison with MCF7 cells stimulated with 1mM of H_2O_2 (control ~7%). Nevertheless, the percentage cell death increases massively up to 60% along with decreasing viability by half, as already described. Several studies have revealed that cell apoptosis can be induced by H_2O_2 [26-29]. In the present study it was seen that after six hours of H_2O_2 stimulation, oxidative stress was induced along with some cell death for both cell lines (3T3 and MCF7). Both cell lines treated with 1 mM of H_2O_2 expressed high levels of apoptotic and dead cells. Nevertheless, cells under simultaneous treatment underwent a significant decrease in the percentage of both apoptotic and dead cells.

Overall, simultaneous treatment for both cell types has a protective effect presenting lower percentages of dead cells comparing to cells that were treated with only 1 mM H_2O_2. MCF7 seems to have a specific intricate protective mechanism in the presence of the PLGA-Col-MnO_2 microspheres as the percentage of apoptotic and dead cells is greatly reduced. With regard to 3T3 cells, simultaneous treatment had a protective effect by reducing the percentage of dead cells but not the percentage of apoptotic cells which is significantly increased. Thus, the simultaneously treated group with H_2O_2 and the microspheres did not prevent apoptosis but did prevent cell death. Analysis of the data from the pre-treated groups for both cell types revealed a lower protective effect for MCF7 cells was observed where the percentage of apoptotic cells was reduced, however the percentage of dead cells was increased. No protective effect of the microspheres was revealed in a harsh environment for this cell type. However, for 3T3 cells, there was a slight increase in apoptotic cells in comparison to the group that was treated only with H_2O_2, whilst the percentage of dead cells did not change significantly. Our data showed that the highly specific cell mechanism by which oxidative stress induced by ROS, specifically H_2O_2, is mediated is dependent on a wide number of factors and conditions, including cell type, the environment, dosage and contact time [28].

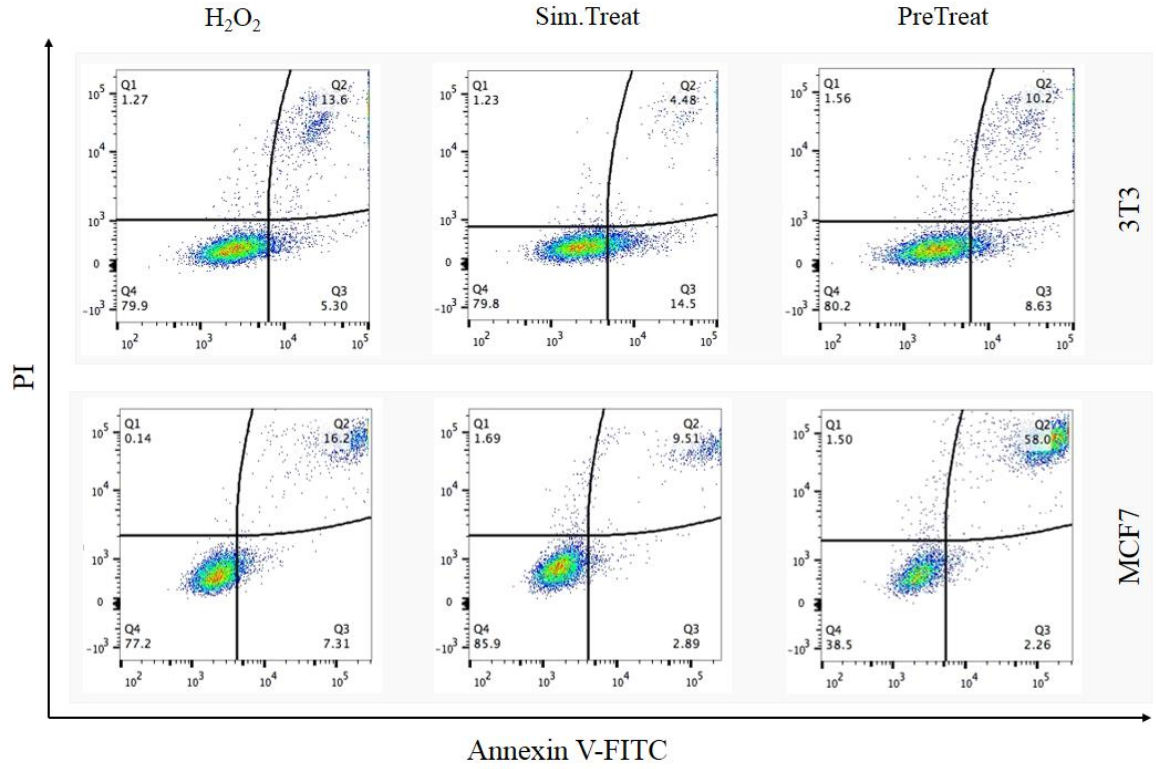

Figure 6: Effect of PLGA-Col-MnO_2 microspheres on cell viability, apoptosis and death. Flow cytometric analysis of Annexin V-FITC on 3T3 cell line and MCF7 cell line 6h after treatment.

4. Discussion

The overproduction of ROS and the subsequent oxidative stress that cells in diseased areas undergo, is thought to be involved in the development of various diseases including, cancer, myocardial infarction, atherosclerosis, diabetes, Alzheimer's disease and other cerebrovascular, cardiovascular and neurodegenerative disorders. The current treatments for oxidative stress are limited to preventive strategies and the use of anti-oxidants, which in most cases are not enough to lead to the regression of a disease. The use of nanostructures able to respond to ROS by altering their morphological characteristics, resulting to a control release of therapeutic molecules, and/or ROS scavengers, render these nanostructures as potential candidates against oxidative stress. Knowing that MnO_2 has the ability to decompose H_2O_2 to water and oxygen, a few studies have been presented showing its therapeutic effect. The decomposition of H_2O_2 can result in the reduction of ROS and the subsequent reduction in the H_2O_2-mediated apoptosis that is observed in cells under oxidative stress. However, it has to be noted that ROS-based therapies are still under investigation because the biological basis of this approach states that higher endogenous ROS levels in cells, undergoing imbalanced oxidative stress, is the basis for therapeutic strategies either to selectively induce or inhibit ROS production. Therefore, ROS scavenging systems have also been reported in the literature as having beneficial outcomes[15, 30]. Our study supports the hypothesis that PLGA-Col-MnO_2 microspheres are able to attenuate H_2O_2-mediated apoptosis by scavenging the overexpressed ROS. The anti-apoptotic effect due to the H_2O_2 scavenging mechanism of the microspheres might be exerted via interconnected pathways, extrinsic and intrinsic, mediated by death receptors and by mitochondria. Nevertheless, further studies need to be undertaken for a full understanding of the endogenous mechanism by which the reported MnO_2-based systems exhibit potential as a therapeutic intervention.

In this study, PLGA microspheres cloaked with collagen type I and decorated with MnO_2 nanoparticles were successfully fabricated. The spheres acted as ROS scavengers, for varying concentrations of H_2O_2 while simultaneously increasing O_2 levels in a control manner. In addition, it was demonstrated that O_2 generated due to the scavenging effect depended not only on the concentration of H_2O_2 but also on the concentration of the spheres. In this study, extreme conditions of oxidative stress were used *in vitro* to prove that the PLGA-Col-MnO_2 microspheres are able to protect cells and the results demonstrated that the microspheres provided a protective effect to cells even in highly ROS-induced environments. Furthermore, the mechanisms by which microspheres controlled apoptosis and cell death was not only cell type specific but also temporal and dosage-dependent.

Acknowledgements

The authors also acknowledge Diana R. Pereira for her assistance with the experimental design and analysis of flow cytometry results.

References

1. Valko M, Leibfritz D, Moncol J, Cronin MT, Mazur M, Telser J. Free radicals and antioxidants in normal physiological functions and human disease. *Int J Biochem Cell Biol*. 2007;**39**:44-84.
2. Rhee SG. Redox signaling: hydrogen peroxide as intracellular messenger. *Exp Mol Med*. 1999;**31**:53-9.
3. Lee D, Bae S, Hong D, Lim H, Yoon JH, Hwang O, et al. H_2O_2-responsive molecularly engineered polymer nanoparticles as ischemia/reperfusion-targeted nanotherapeutic agents. *Sci Rep*. 2013;**3**:2233.
4. Park S, Yoon J, Bae S, Park M, Kang C, Ke Q, et al. Therapeutic use of H_2O_2-responsive anti-oxidant polymer nanoparticles for doxorubicin-induced cardiomyopathy. *Biomaterials*. 2014;**35**:5944-53.
5. Valko M, Rhodes CJ, Moncol J, Izakovic M, Mazur M. Free radicals, metals and antioxidants in oxidative stress-induced cancer. *Chem Biol Interact*. 2006;**160**:1-40.
6. Reuter S, Gupta SC, Chaturvedi MM, Aggarwal BB. Oxidative stress, inflammation, and cancer: how are they linked? *Free Radic Biol Med*. 2010;**49**:1603-16.
7. Lin MT, Beal MF. Mitochondrial dysfunction and oxidative stress in neurodegenerative diseases. *Nature*. 2006;**443**:787-95.
8. Poole KM, Nelson CE, Joshi RV, Martin JR, Gupta MK, Haws SC, et al. ROS-responsive microspheres for on demand antioxidant therapy in a model of diabetic peripheral arterial disease. *Biomaterials*. 2015;**41**:166-75.
9. Tapeinos C, Pandit A. Physical, chemical, and biological structures based on ROS-sensitive moieties that are able to respond to oxidative microenvironments. *Adv Mater*. 2016;**28**:5553-85.

10. Tanner P, Balasubramanian V, Palivan CG. Aiding nature's organelles: artificial peroxisomes play their role. *Nano Lett*. 2013;**13**:2875-83.
11. Spulber M, Baumann P, Liu J, Palivan CG. Ceria loaded nanoreactors: a nontoxic superantioxidant system with high stability and efficacy. *Nanoscale*. 2015;**7**:1411-23.
12. Li J, Shu Y, Hao T, Wang Y, Qian Y, Duan C, et al. A chitosan-glutathione based injectable hydrogel for suppression of oxidative stress damage in cardiomyocytes. *Biomaterials*. 2013;**34**:9071-81.
13. Louzao I, van Hest JC. Permeability effects on the efficiency of antioxidant nanoreactors. *Biomacromolecules*. 2013;**14**:2364-72.
14. Song M, Liu T, Shi C, Zhang X, Chen X. Bioconjugated manganese dioxide nanoparticles enhance chemotherapy response by priming tumor-associated macrophages toward M1-like phenotype and attenuating tumor hypoxia. *ACS Nano*. 2016;**10**:633-47.
15. Gordijo CR, Abbasi AZ, Amini MA, Lip HY, Maeda A, Cai P, et al. Design of hybrid MnO_2-polymer-lipid nanoparticles with tunable oxygen generation rates and tumor accumulation for cancer treatment. *Adv Funct Mater*. 2015;**25**:1858-72.
16. Prasad P, Gordijo CR, Abbasi AZ, Maeda A, Ip A, Rauth AM, et al. Multifunctional albumin-MnO_2 nanoparticles modulate solid tumor microenvironment by attenuating hypoxia, acidosis, vascular endothelial growth factor and enhance radiation response. *ACS Nano*. 2014;**8**:3202-12.
17. Luo XL, Xu JJ, Zhao W, Chen HY. A novel glucose ENFET based on the special reactivity of MnO_2 nanoparticles. *Biosens Bioelectron*. 2004;**19**:1295-300.
18. Hasan MA, Zaki MI, Pasupulety L, Kumari K. Promotion of the hydrogen peroxide decomposition activity of manganese oxide catalysts. *Appl Catal A-Gen*. 1999;**181**:171-9.

19. Jain RA. The manufacturing techniques of various drug loaded biodegradable poly(lactide-co-glycolide) (PLGA) devices. *Biomaterials*. 2000;**21**:2475-90.
20. Thomas D, Fontana G, Chen X, Sanz-Nogues C, Zeugolis DI, Dockery P, et al. A shape-controlled tuneable microgel platform to modulate angiogenic paracrine responses in stem cells. *Biomaterials*. 2014;**35**:8757-66.
21. Browne S, Monaghan MG, Brauchle E, Berrio DC, Chantepie S, Papy-Garcia D, et al. Modulation of inflammation and angiogenesis and changes in ECM GAG-activity via dual delivery of nucleic acids. *Biomaterials*. 2015;**69**:133-47.
22. Newland B, Moloney TC, Fontana G, Browne S, Abu-Rub MT, Dowd E, et al. The neurotoxicity of gene vectors and its amelioration by packaging with collagen hollow spheres. *Biomaterials*. 2013;**34**:2130-41.
23. Yao L, Billiar KL, Windebank AJ, Pandit A. Multichanneled collagen conduits for peripheral nerve regeneration: design, fabrication, and characterization. *Tissue Eng Part C Methods*. 2010;**16**:1585-96.
24. Zeugolis DI, Li B, Lareu RR, Chan CK, Raghunath M. Collagen solubility testing, a quality assurance step for reproducible electro-spun nano-fibre fabrication. A technical note. *J Biomater Sci Polym Ed*. 2008;**19**:1307-17.
25. Zeugolis DI, Paul RG, Attenburrow G. Factors influencing the properties of reconstituted collagen fibers prior to self-assembly: animal species and collagen extraction method. *J Biomed Mater Res A*. 2008;**86**:892-904.
26. Martin G, Andriamanalijaona R, Mathy-Hartert M, Henrotin Y, Pujol JP. Comparative effects of IL-1beta and hydrogen peroxide (H_2O_2) on catabolic and anabolic gene expression in juvenile bovine chondrocytes. *Osteoarthritis Cartilage*. 2005;**13**:915-24.

27. Ferreira Mendes A, Caramona MM, Carvalho AP, Lopes MC. Hydrogen peroxide mediates interleukin-1β-induced AP-1 activation in articular chondrocytes: Implications for the regulation of iNOS expression. *Cell Biol Toxicol*. 2003;**19**:203-14.
28. Zhu C, Hu W, Wu H, Hu X. No evident dose-response relationship between cellular ROS level and its cytotoxicity-a paradoxical issue in ROS-based cancer therapy. *Sci Rep*. 2014;**4**:5029.
29. Yang L, Rong Z, Zeng M, Cao Y, Gong X, Lin L, et al. Pyrroloquinoline quinone protects nucleus pulposus cells from hydrogen peroxide-induced apoptosis by inhibiting the mitochondria-mediated pathway. *Eur Spine J*. 2015;**24**:1702-10.
30. Kim CK, Kim T, Choi IY, Soh M, Kim D, Kim YJ, et al. Ceria nanoparticles that can protect against ischemic stroke. *Angew Chem Int Ed Engl*. 2012;**51**:11039-43.

Supplementary Information

Functionalised collagen spheres reduce H_2O_2 mediated apoptosis by scavenging overexpressed ROS

Fabrication of MnO_2 nanoparticles and decoration efficiency

The MnO_2 nanoparticles were fabricated using a modified previously described procedure.[1,2] Briefly, poly allylamine hydrochloride and potassium permanganate were dissolved in distilled water and left under stirring for 16 hours. The solution was then freeze dried and after freeze drying five washings with distilled water were carried out. The nanoparticles were collected by centrifugation at 8000 rpm for 30 min and at 4 °C. During the fabrication procedure of the MnO_2 nanoparticles a thin layer of poly allylamine hydrochloride is created. The free amine groups around the nanoparticles can covalently bond to the activated groups of PLGA but can also electrostatically interact with collagen's carboxylic groups. Even though this specific property enhances the entrapment efficiency of the nanoparticles, the NHS groups on the surface of the microspheres plays important role in this entrapment. The emulsion method that is used for the fabrication of the microspheres does not allow to control the number of the functional group on the surface making it difficult to know the exact amount of MnO_2 nanoparticles that will decorate the surface. However, after repeating the experimental procedure numerous times and after optimizing the fabrication and decoration protocol, we have seen that using the specific reagents and the specific amounts that are described below, the final concentration of the MnO_2 nanoparticles ranges from 4.5 – 5.0 wt% of the final product. Lower and higher concentrations have also been used during the

[1] Gordijo CR, Abbasi AZ, Amini MA, Lip HY, Maeda A, Cai P, et al. Design of hybrid MnO_2-polymer-lipid nanoparticles with tunable oxygen generation rates and tumor accumulation for cancer treatment. *Adv Funct Mater*. 2015;**25**:1858-72.

[2] Prasad P, Gordijo CR, Abbasi AZ, Maeda A, Ip A, Rauth AM, et al. Multifunctional albumin-MnO_2 nanoparticles modulate solid tumor microenvironment by attenuating hypoxia, acidosis, vascular endothelial growth factor and enhance radiation response. *ACS Nano*. 2014;**8**:3202-1

decoration procedure of the microspheres but lower concentrations resulted in an inadequate scavenging effect while higher concentrations resulted in an excess amount of nanoparticles that could not be entrapped.

Dose Selection

MnO*2* nanoparticles:

MnO_2 nanoparticles interact with the collagen solution and enhance its gelation depending on their concentration. The dose was selected considering the highest concentration of MnO_2 nanoparticles that is needed in order to protect the cells, by scavenging the H_2O_2, and at the same time the lowest in order to avoid gelation of the collagen solution during the coating procedure.

***In vitro* studies:**

In *in vitro* studies the doses were selected taking into consideration the highest scavenging effect but at the same time the lowest cytotoxicity. Higher doses than the selected ones had the same effect in the scavenging of H_2O_2 but the cytotoxicity of the microspheres was increased. Thus, we used the optimum concentrations that are presented in the manuscript.

H_2O_2 in *in vitro* studies:

Various amounts of H_2O_2 have been tested *in vitro* but the specific concentration(1mM) was chosen because we wanted to study how the cells respond to extreme conditions of oxidative stress. Lower concentrations (<500uM) didn't affect drastically the metabolic activity of the cells, since the protective mechanisms of the cells were able to scavenge the majority of the added H_2O_2, while amounts higher than 1mM led to the immediate death of the cells.

Activation of PLGA and microspheres fabrication

Poly(D,L-lactide-co-glycolide) (PLGA) was activated using carbodiimide chemistry. Briefly, PLGA (200 mg, 0.00432 mmol) was dissolved in 3 ml of dichloromethane and while stirring EDC (13.5 mg, 0.0864 mmol) was added to the solution. After stirring for ten minutes, NHS (9.94 mg, 0.0864 mmol) was also added, and the solution was left for twelve hours at room temperature to react. For the fabrication of the spheres, PLGA-NHS (25mg) was dissolved in 0.5ml of DCM and was added to a poly (vinyl alcohol) (PVA) solution (1% w/v). The resulting solution was instantly homogenized at 13,000 rpm for three minutes and then left for eight hours under mild stirring at room temperature for DCM to evaporate. The spheres were collected by spinning at 1,000 rpm for five minutes and washed four times with distilled H_2O. The activated PLGA-NHS microspheres (25mg) were dispersed in PBS (1x) (1 ml) to which 0.2 ml of MnO_2 nanoparticles (initial concentration: 10 mg/ml in acetic acid 0.5M) were added while stirring. 1 ml of a collagen solution (initial concentration: 5mg/ml in acetic acid 0.5 M) was diluted with 7.8 ml of PBS (1x) and the resulting collagen solution was added drop wise to the PLGA-NHS-MnO_2 solution. The pH was adjusted to 7.4 using NaOH (10M). After twelve hours the final product was collected by spinning at 1,000 rpm for five minutes and washed four times with acetic acid 0.5M (**Figure 1**).

Transmission electron microscopy analysis

Transmission electron microscopy was used to characterize the size and shape of the MnO_2 nanoparticles. As seen in Figure S1, the spherical nanoparticles' size is around 15 nm.

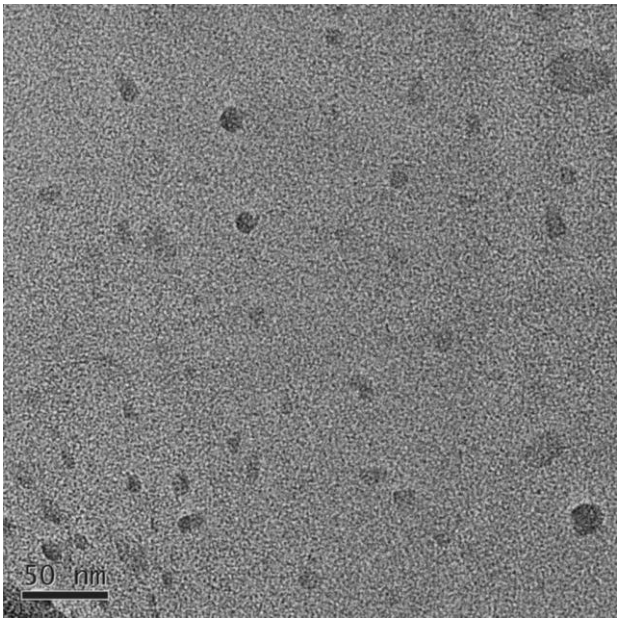

Figure S1. TEM image of the fabricated spherical (15 nm) MnO_2 nanoparticles; Scale Bar: 50 nm

Fourier-transformed infrared spectroscopy

The MnO_2 nanoparticles as well as the functionalized PLGA-Collagen-MnO_2 microspheres were characterized using Fourier transform infrared spectroscopy (FT-IR) spectroscopy (**Figure S2**). Because of the strong bands of PLGA and the overlapping between some of the peaks of collagen and PLGA, no evident differences except in the peaks ranging from 1500-1600 cm^{-1} that can be attributed to N-H bonds, were observed. The same peaks of the spectrum for MnO_2 nanoparticles were attributed to N-H bonds since during their fabrication poly (allyl amine) hydrochloride was used to stabilise the MnO_2 nanoparticles. The peak at 420 cm^{-1} that is observed to the MnO_2 nanoparticles spectrum (**Figure S2-top**) as well as to the spectrum of the final product (PLGA-Col-MnO_2 microspheres) (**Figure S2-bottom**) can be attributed to the Mn-O vibration and is indicative of the incorporation of the nanoparticles on the surface of the PLGA-Col-MnO_2 microspheres. The presence of the MnO_2 nanoparticles was also verified using electron diffraction x-ray (EDX) analysis and it was found that Mn represented approximately ~5 wt% of the PLGA-Collagen microspheres

(**Figure S3)**. Before the fabrication of the microspheres, PLGA presenting carboxylic acid terminal groups was activated using carbodiimide chemistry and characterized using ^{1}H NMR as it can be seen in **Figure S4**. This functionalization enabled the use of the activated groups on the microsphere surface as an anchor for the conjugation with the amine groups of the collagen to enhance its stability as an external layer.

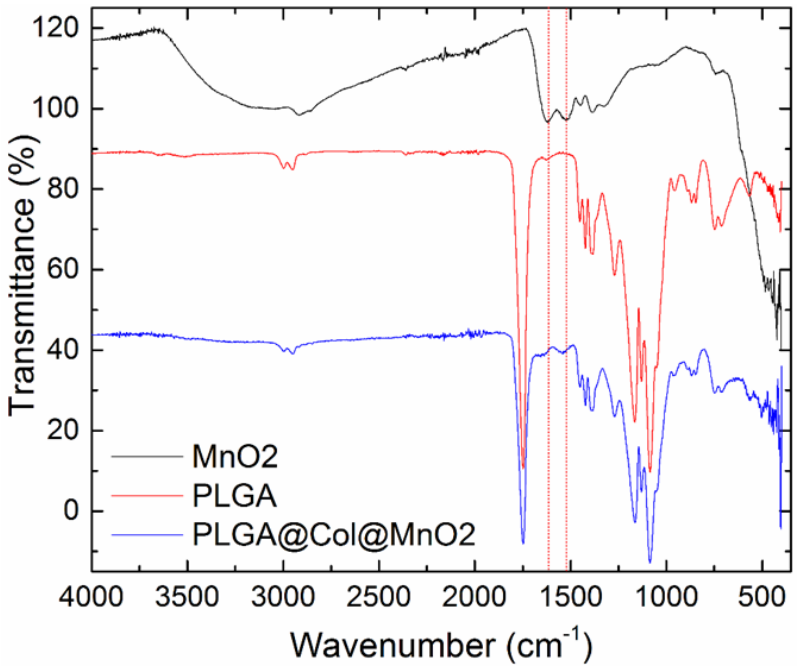

Figure S7: FT-IR specta of MnO_2 nanoparticles **(top)**, PLGA **(middle)** and PLGA-Col-MnO_2 microspheres **(bottom)**.

Electron dispersion X-ray analysis

The percentage of manganese on the surface of the collagen nanospheres was calculated using electron dispersion x-ray analysis and the results are given in **Figure S3**. The amount of Mn was 5 % per weight. The peaks around 1.8 and 2.2 KeV are due to gold coating during the preparation of the samples.

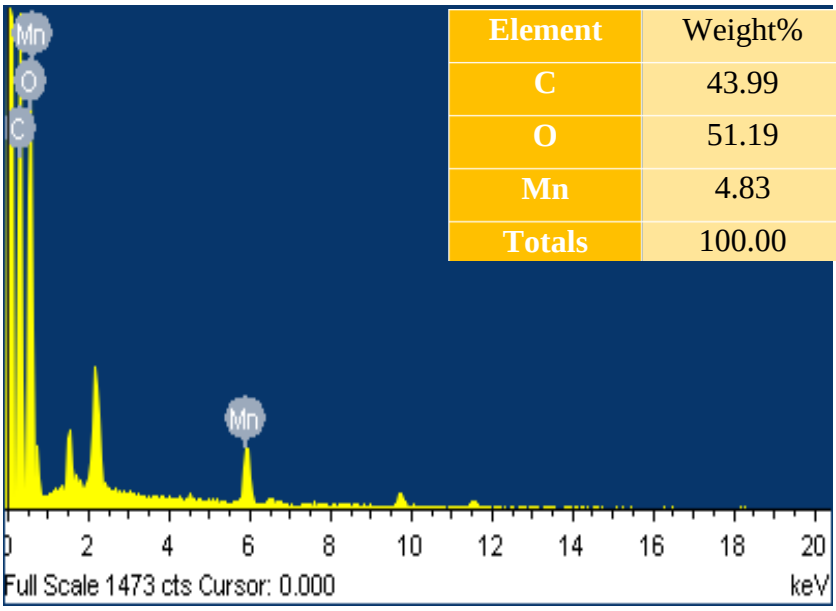

Element	Weight%
C	43.99
O	51.19
Mn	4.83
Totals	100.00

Figure S3. EDX analysis of the PLGA-Col-MnO_2 microspheres after incorporating MnO_2 nanoparticles

^{1}H Nuclear magnetic resonance analysis

The characterization of the activated PLGA was carried out using NMR spectroscopy. ^{1}H NMR (400 MHz, $CDCl_3$): δ 4.27 (-NCH2CH2-), 3.64 (s, (-CH2CH2O-), 2.62 (-NCH_2CH_2-CONH-), 1.6 (-OCH(CH_3) CONH-) ppm.

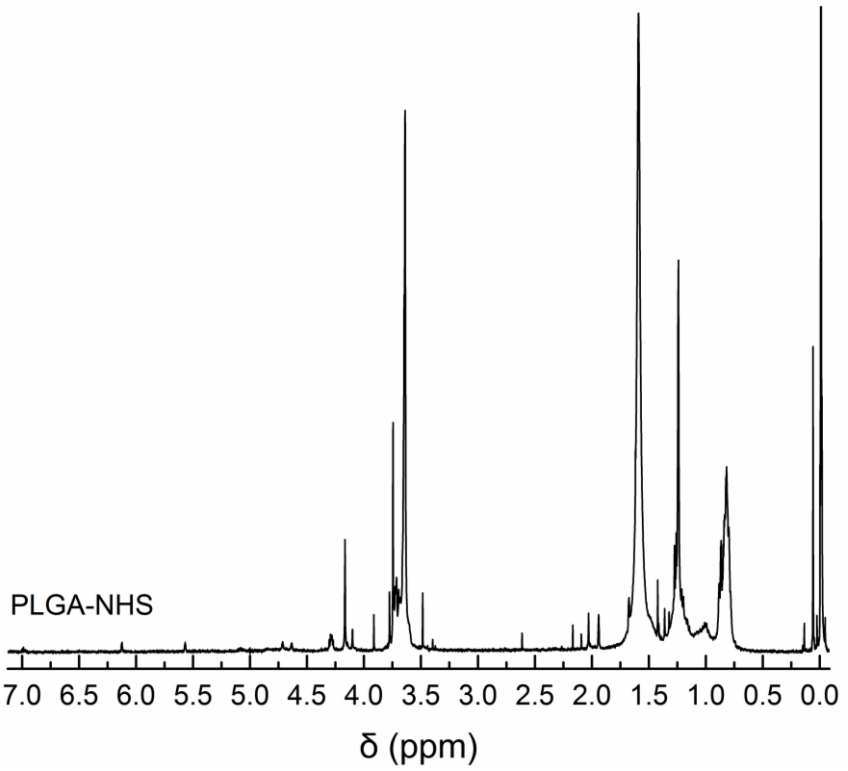

Figure S4. ^{1}H NMR spectrum of the activated PLGA

Kinetic studies

To evaluate how the endogenous production of ROS is affected in inflamed cells under oxidative stress, a kinetic study to evaluate the intracellular production of ROS was carried out on 3T3 and MCF7 cells. In this experiment, cells were stimulated with varying concentrations (10, 50 or 100 ng/ml) of IL-1β and varying concentrations of H_2O_2 (50 or 500 μM). The kinetic studies were carried out for six hours due to the limitation in the activity of the DCFDA dye. The intracellular concentration of ROS increased over the course of the experiment as illustrated in **Figure S5**. However, the increase was higher in all the stimulated cells compared to the unstimulated ones. At all-time points for the stimulated 3T3 cells (**Figure S5-A**), the amount of ROS generated endogenously was higher than the unstimulated cells displaying the highest value after six hours, where the ROS concentration in the stimulated cells is ~30% higher than the unstimulated cells. Stimulation with IL-1β (100

ng/ml) also resulted in an increased ROS concentration (~15%) comparing to the untreated cells after six hours, but this concentration was not as intense as the stimulation with H_2O_2 (500 μM) which increased ROS concentration approximately by ~45%. Similar results were observed in MCF7 cells stimulated with H_2O_2 (500 μM) (30% increase in ROS) but a lower increase in ROS (2.5% - 7.0%) was observed for the other groups (**Figure S5-B**), when compared to the MCF7 untreated cells. One possible reason for this difference is that the proliferation rate of MCF7 cells was higher, resulting in higher ROS scavenging activity. This phenomenon cannot be observed after stimulation with high concentrations of H2O2 because the scavenging mechanism of the cells is not powerful enough to scavenge all the generated H2O2. The increase in the endogenous ROS production had an effect on the metabolic activity of the cells as will be discussed in the next section.

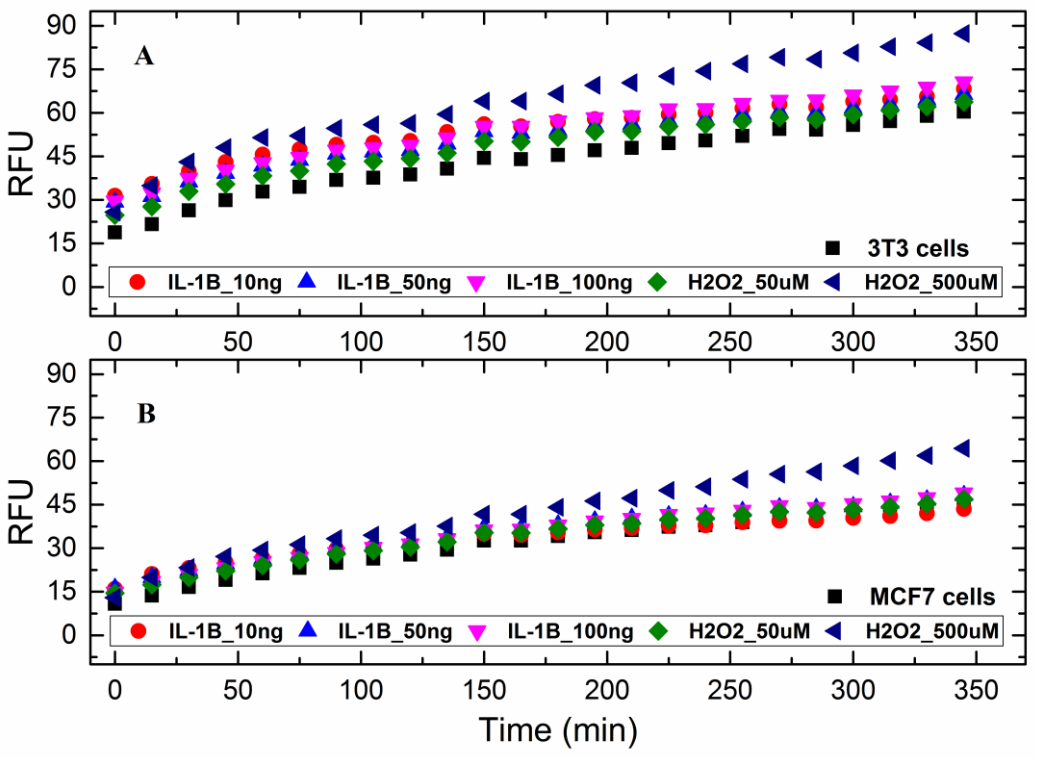

Figure S5. Kinetic studies on **A)** 3T3 and **B)** MCF7 cells, untreated (■) or treated with IL-1β: 10 ng/ml (●), IL-1β: 50 ng/ml (▲), IL-1β: 100 ng/ml (▼), H2O2: 50 μM (♦) and H2O2: 500 μM (◀) for 6h.

Cellular metabolic activity and proliferation using AlamarBlue®

In brief, after each time point of each experiment, cell culture media was aspirated and the cells were washed twice with HBSS. A 10% AB solution in culture media (without phenol red and FBS) was added to each well and incubated for three hours at 37º C. AB absorbance was read using a microplate reader at wavelengths of 540 nm and 595nm. Three replicates per experiment were performed and the results were averaged. Wells containing only AB solution and only media were also prepared. The fluorescence measured in the latter was used as a background and to calculate the correlation factor. In order to calculate the percentage of alamarBlue® reduction, the following formula was applied:

$$\%\ Alamar\ blue\ reduction = (A_{LW} - (A_{Hw} \times R_0)) \times 100\ ;$$

Where, A_{LW} is the absorbance at low wavelength, A_{HW} is the absorbance at high wavelength and R_0 is the correlation factor.

$$R_0\ =\ AO_{LW}/AO_{HW}\ ;$$

Where, AO_{LW} is the subtraction of AB solution to the media only at low wavelength absorbance and AO_{HW} is the subtraction of AB solution from the media at high wavelength absorbance.

Subsequently the medium was removed and washed three times with Hank's Balanced Salt Solution (HBSS) to remove all the dye solution. At each well 1ml of Milli-Q ultrapure water was added followed by the scraping of each surface with the tip of a pipette. The solution was transferred to an eppendorf and frozen at -80º C. Then, samples were thawed and the DNA amount was measured using the Quant-iT PicoGreen® dsDNA assay Kit (Invitrogen) according to the manufacturer's instructions. Samples were incubated, in a 96 opaque plate, with PicoGreen® dye, protected from light for ten minutes, and fluorescence signals

(excitation 484 nm, emission 520 nm) detected using a fluorescence microplate reader. A standard curve was developed using a λDNA standard, provided with the kit. The standard curve was within the range of 10ng/ml to 2 μg/ml λDNA and was used to calculate the final DNA content per millilitre of sample. A Perkin Elmer enzyme-linked immunosorbent assay (ELISA) plate reader was used for the proliferation and metabolic activity measurements. Excitation and emission values were set according to the protocols of each assay.

Protective effect of PLGA-Col-MnO_2 microspheres on H_2O_2-induced cytotoxicity

The effect of the PLGA-Col-MnO_2 microspheres on the metabolic activity of the 3T3 and MCF7 cell lines was assessed for varying microspheres concentrations for a time period up to 72 hours. In **Figure S6** it was demonstrated that the cells metabolic activity was independent of microspheres concentrations up to 500 μg/ml, a concentration which was also used to assess the O_2 generation capacity and the ROS scavenging effect of the microspheres. Cellular metabolic activity was measured under stimulation with different concentrations of H_2O_2 as well as at different concentrations of PLGA-Col-MnO_2 microspheres as shown in **Figure S6-A** and **Figure S6-B**. For the lower concentrations of H_2O_2 (from 500μM to 100 μM), no significant differences in cell metabolic activity were observed for the different cell lines for up to six hours.

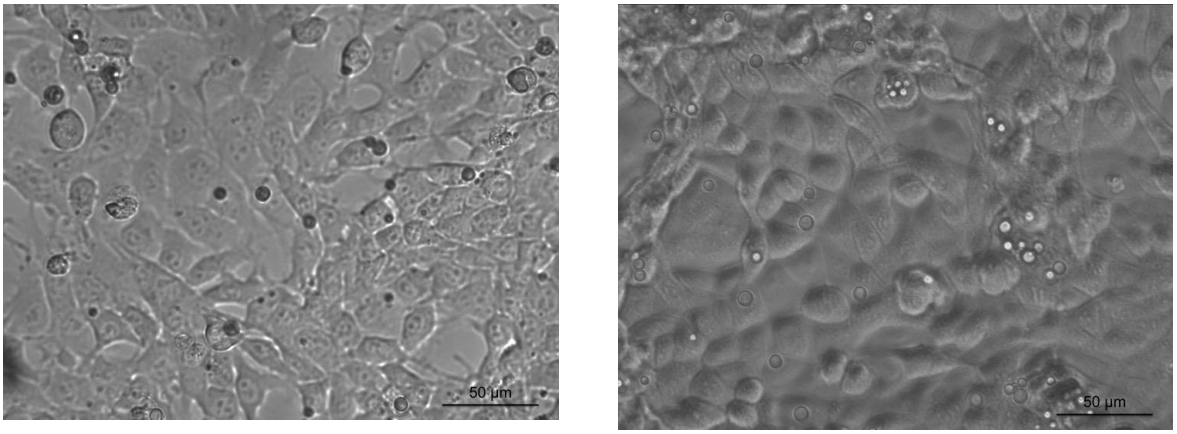

A **B**

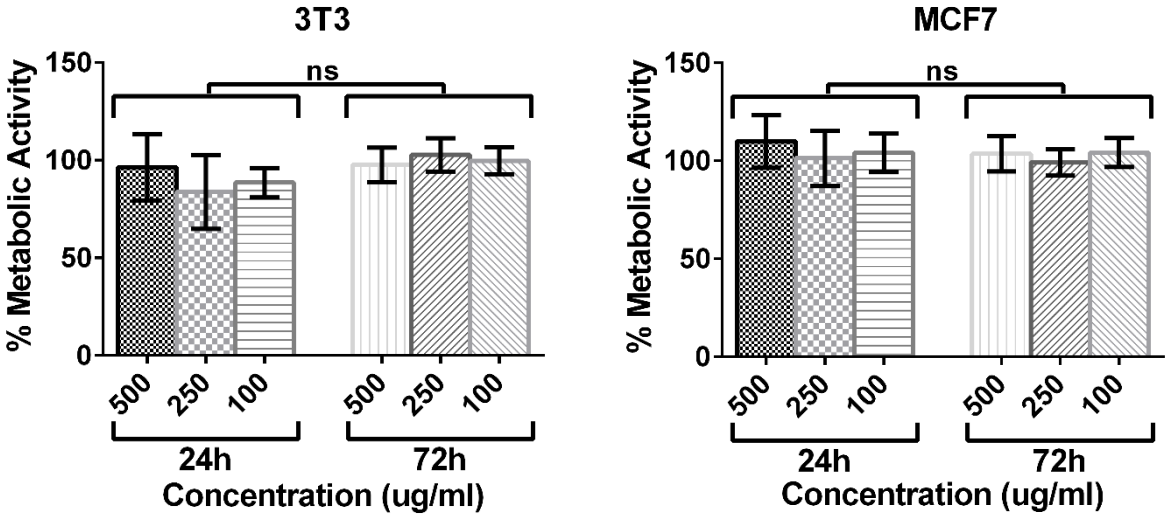

C **D**

Figure S6: Optical images of **A)** 3T3 cells after treatment with 100 µg/ml PLGA-Col-MnO_2 microspheres for 24h, **B)** MCF7 cells after treatment with 100 µg/ml PLGA-Col-MnO_2 microspheres for 72h, **C)** 3T3 cell metabolic activity using different concentrations of PLGA-Col-MnO_2 microspheres for 24h and 72h (n=3, ANOVA, ns: no significant difference, p<0.05).and **D)** MCF7 cells metabolic activity using different concentrations of PLGA-Col-MnO_2 microspheres for 24h and 72h (n=3, ANOVA, ns: no significant difference, p<0.05).

In contrast, when cells were stimulated with higher concentrations of H_2O_2 (1 mM), their metabolic activity was reduced. Further studies were performed by stimulating cells with 1 mM of H_2O_2 to induce oxidative stress on the cells.

In order to correlate this H_2O_2 concentration with the *in vivo* constant generation of H_2O_2 which is responsible for the oxidative stress, we conducted a simple experiment where we treated both cell types with repeated additions of 50 μM of H_2O_2 for six hours every 36 minutes. The results presented in **Figure S7** demonstrate that the effect of the repetitive addition of 50 μM of H_2O_2 is comparable to the effect of the one-time induction of 1 mM of H_2O_2.

A significant difference was observed in the metabolic activity of healthy cells, cells stimulated with H_2O_2 only, and cells stimulated with H_2O_2 but in the presence of PLGA-Col-MnO_2 microspheres. Both cell lines were stimulated with H_2O_2 prior to the addition of PLGA-Col-MnO_2 microspheres utilising both Sim.Treat or Pre-treat treatment regimes. The results presented in **Figure S7-C** demonstrate the protective effect of the microspheres on the metabolic activity of 3T3 cells due to H_2O_2 scavenging. When cells under oxidative stress were treated with the PLGA-Col-MnO_2 microspheres, their metabolic activity was higher compared to cells stimulated only with H_2O_2. A significant difference was also observed between the Sim.Treat and the Pre-treat treatment regimes. In the Pre-treat regime, cells demonstrated lower metabolic activity than for cells treated using the Sim.Treat treatment regime. This indicates that the high concentration of H_2O_2 in the Pre-treat regime may lead to oxidative stress that cells cannot revert. Furthermore, the low concentration of the microspheres (100 μg/ml) does not appear to offer a protective effect against H_2O_2.

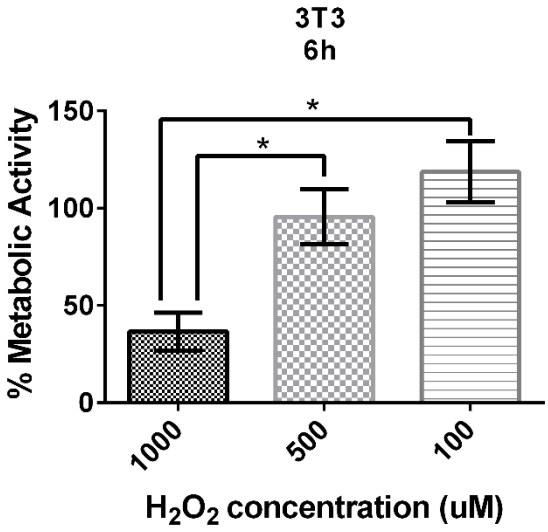
3T3
6h
% Metabolic Activity
150
100
50
0
*
*
1000
500
100
H2O2 concentration (uM)

A

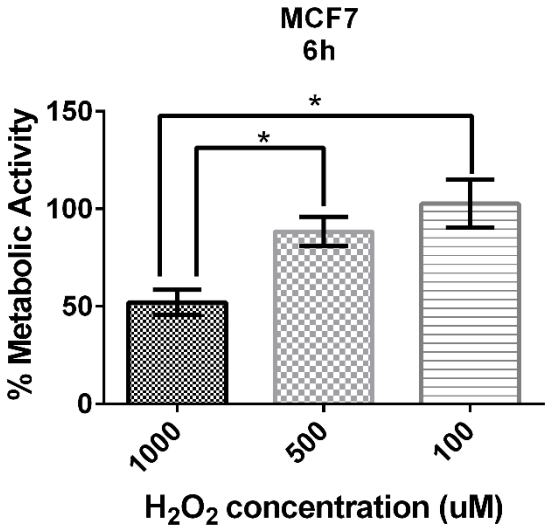
MCF7
6h
% Metabolic Activity
150
100
50
0
*
*
1000
500
100
H2O2 concentration (uM)

B

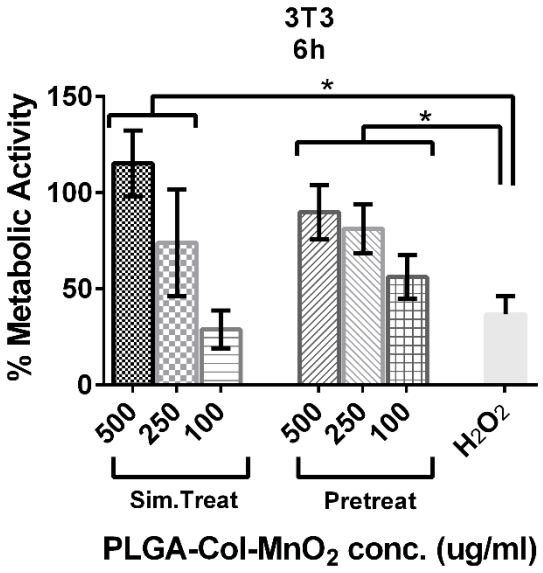
3T3
6h
% Metabolic Activity
150
100
50
0
*
*
500
250
100
500
250
100
H2O2
Sim.Treat
Pretreat
PLGA-Col-MnO2 conc. (ug/ml)

C

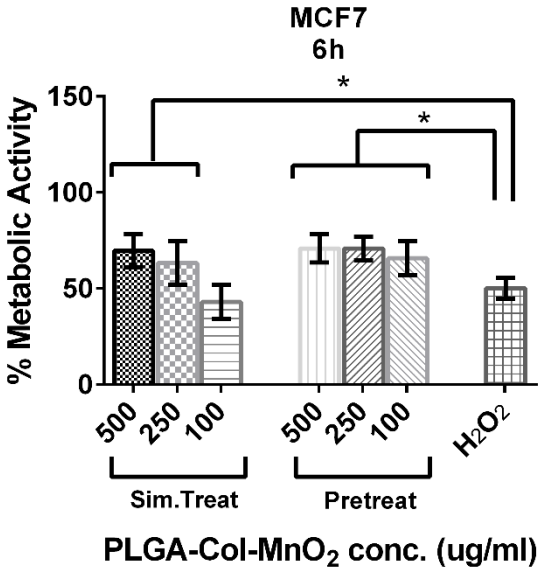
MCF7
6h
% Metabolic Activity
150
100
50
0
*
*
500
250
100
500
250
100
H2O2
Sim.Treat
Pretreat
PLGA-Col-MnO2 conc. (ug/ml)

D

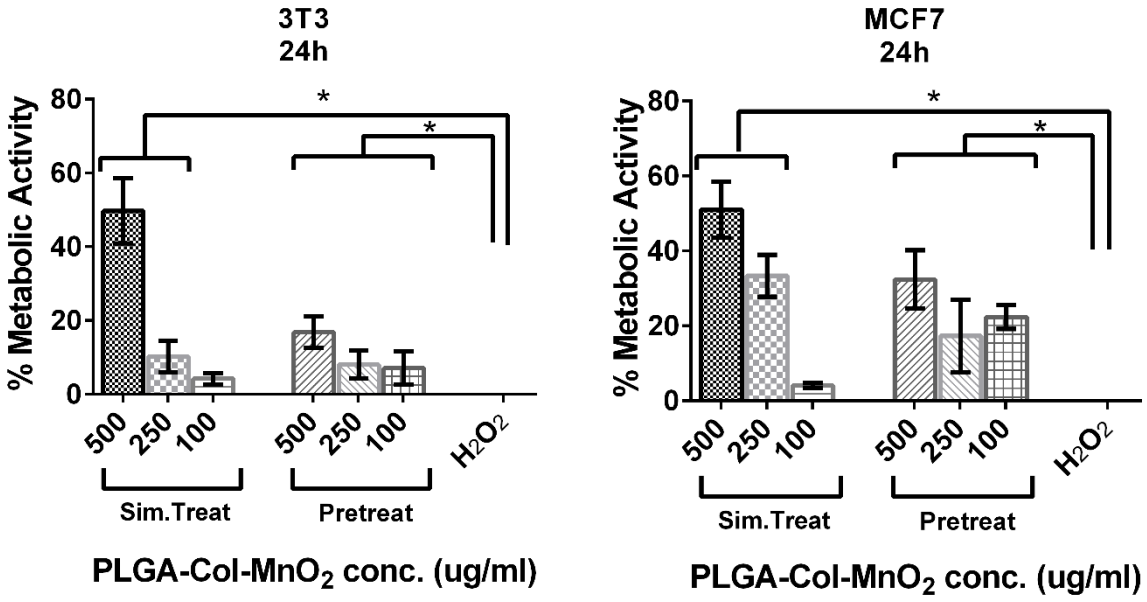

E **F**

Figure S7: Cell metabolic of **A)** 3T3 and **B)** MCF7 cell lines under stimulation with 100 μM, 500 μM and 1 mM of H_2O_2 for 6h. Significant difference was observed in the groups stimulated with 1 mM of H_2O_2 compared to the other two groups. (n=3, ANOVA, $p<0.05$). Cells metabolic activity on **C)** 3T3 cells for 6h and **D)** MCF7 cells for 6h and **E)** 3T3 cells for 24 hours and **F)** MCF7 cells for 24h. All cells underwent oxidative stress by stimulation with 1 mM of H_2O_2. For each set of experiments, two different treatments regimes were applied: Sim.Treat and Pre-treat. Significant difference was observed in the groups stimulated with 1mM of H_2O_2 when compared to the groups treated with PLGA-Col-MnO_2 microspheres using either the Sim.Treat or Pre-treat treatment regimes. (n=3, ANOVA, *→$p<0.05$). Data was normalized to unstimulated cells.

A similar but not as pronounced an effect was also observed in MCF7 cells as shown in **Figure S7-D**. MCF7 cells presented higher metabolic activity towards H_2O_2 than in 3T3 cells which was probably due to their increased tolerance in reactive oxygen species produced from exogenous stress [3, 4]. In **Figures S7-E** and S7-**F,** it was evident that cells

which underwent the Sim.Treat treatment regime and microspheres (500 μg/ml) present a higher metabolic activity than in cells that were stimulated only with H_2O_2. This phenomenon can be seen as a protective effect of the PLGA-Col-MnO_2 microspheres. This protective effect can also be observed in the Sim.Treat treatment regime but it is less evident than in the Pre-treat treatment regime. Such a high level of H_2O_2 overwhelms the scavenging ability of the microspheres and therefore the protective effect is not seen for the Pre-treat treatment regime. Additionally, the protective effect of the microspheres in the MCF7 cells, after 24h, was demonstrated only for concentrations of 500 μg/ml or 250 μg/ml. It has to be noted that the protective effect in this cell type is sub-veined by the increased tolerance of this cell line to increased ROS.

Mimicking the effect of oxidative stress

To mimic the effect of oxidative stress on the cellular metabolic activity is seen in diseased state, cells were given repeated treatments of 50 μM H_2O_2 and these results were compared to the data obtained from a single treatment of 1,000 uM. The results presented in Figure S6 demonstrates that repeated treatments with 50 uM of H_2O_2 has a similar resulting data as treating cells once with 1000 uM of H_2O_2. It has to be noted that, 50 uM of H_2O_2 is the concentration that is generated intracellularly in cells under oxidative stress conditions.

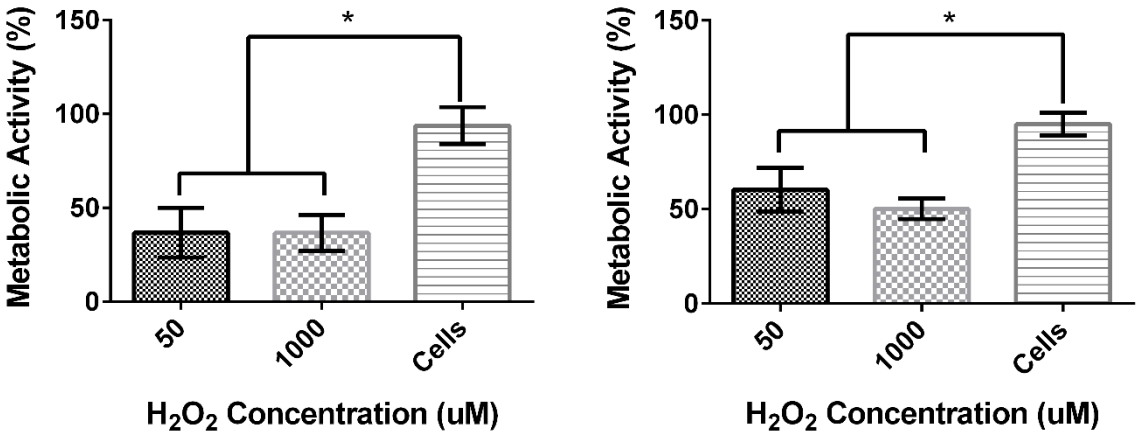

A **B**

Figure S8. Cells' metabolic activity on **A)** 3T3 fibroblasts and **B)** MCF-7 cancer cells after inducing oxidative stress using 1000 uM in a one-time treatment for six hours and by inducing oxidative stress by repeated additions of 50 uM of H_2O_2 every 36 minutes for six hours.

References

1. Gordijo CR, Abbasi AZ, Amini MA, Lip HY, Maeda A, Cai P, et al. Design of hybrid MnO_2-polymer-lipid nanoparticles with tunable oxygen generation rates and tumor accumulation for cancer treatment. *Adv Funct Mater*. 2015;**25**:1858-72.
2. Prasad P, Gordijo CR, Abbasi AZ, Maeda A, Ip A, Rauth AM, et al. Multifunctional albumin-MnO_2 nanoparticles modulate solid tumor microenvironment by attenuating hypoxia, acidosis, vascular endothelial growth factor and enhance radiation response. *ACS Nano*. 2014;**8**:3202-12.
3. Tian H, Gao Z, Wang G, Li H, Zheng J. Estrogen potentiates reactive oxygen species (ROS) tolerance to initiate carcinogenesis and promote cancer malignant transformation. *Tumor Biol*. 2016;**37**:141-50.
4. Trachootham D, Alexandre J, Huang P. Targeting cancer cells by ROS-mediated mechanisms: a radical therapeutic approach. *Nat Rev Drug Discov*. 2009;**8**:579-91.